4 Ionosphere and Thermosphere

4-1 Ionospheric Irregularities

MARUYAMA Takashi

Ionospheric irregularities cause scintillations of trans-ionospheric radio waves from satellites. Most severe cases are the scintillations due to plasma bubbles at low latitudes near the magnetic equator, which results in fluctuations of L-band radio signals by 20 dB or more. For the prediction of onsets of plasma bubbles, investigation of a physical mechanism is indispensable. Also precursory phenomena of bubble onsets will be valid for the prediction.

This article describes outstanding problems for the prediction of severe ionospheric scintillations and an ongoing observational approach in CRL.

Keywords
Scintillation, Spread F, Plasma bubble

1 Introduction

The ionospheric irregularities that occur in low-latitude regions near the magnetic equator (called equatorial spread F) are known to disrupt the propagation of radio waves in the frequency range below a few GHz, a band used by navigation and communication systems such as GPS satellites. The spatial irregularities of electron density distributions distort the equi-phase surface of radio waves and lead to irregular variations in electrical field intensity at receiver stations arising from interference between adjacent waves in different phases (Fresnel diffraction). This is the phenomenon known as the ionospheric scintillation. The effects of scintillation arising from equatorial spread F are significant: Cases have been reported of scintillation events exceeding 20 dB in peak-to-peak amplitude fluctuation, even in the L band (see, for example, Kil et al., 2000 ; Fig.1). Intense scintillation causes information loss and phase slips due to lock-off of satellite signals, and studies of the mechanism of equatorial spread F onset are crucial in predicting the occurrence of satellite radio disruption. On one hand, the study of equatorial spread F encompasses a wide range of interests of basic ionospheric studies, including plasma instability, the dynamo effect, and thermosphere-ionosphere coupling. This paper will primarily discuss equatorial plasma instability, with a particular focus on the basic science essential for scintillation prediction.

2 Previous Findings

2.1 The Spread-F

The history of morphological studies of spread F goes back to the days of IGY. In those days, data was obtained mostly from ionosonde observations. Inevitably, the data was limited to data obtained on land at stations with inhomogeneous distributions. Due to this limitation and for lack of knowledge of fundamental mechanisms underlying spread F, most researchers did not treat the equatorial region and the middle-to-high latitude regions as distinct regions. However, even at the time, seasonal variations distinct to each observation point were known to exist, and had led Shimazaki and other researchers to draw a spread-F equator by classifying each observation station as a summer or winter type, based

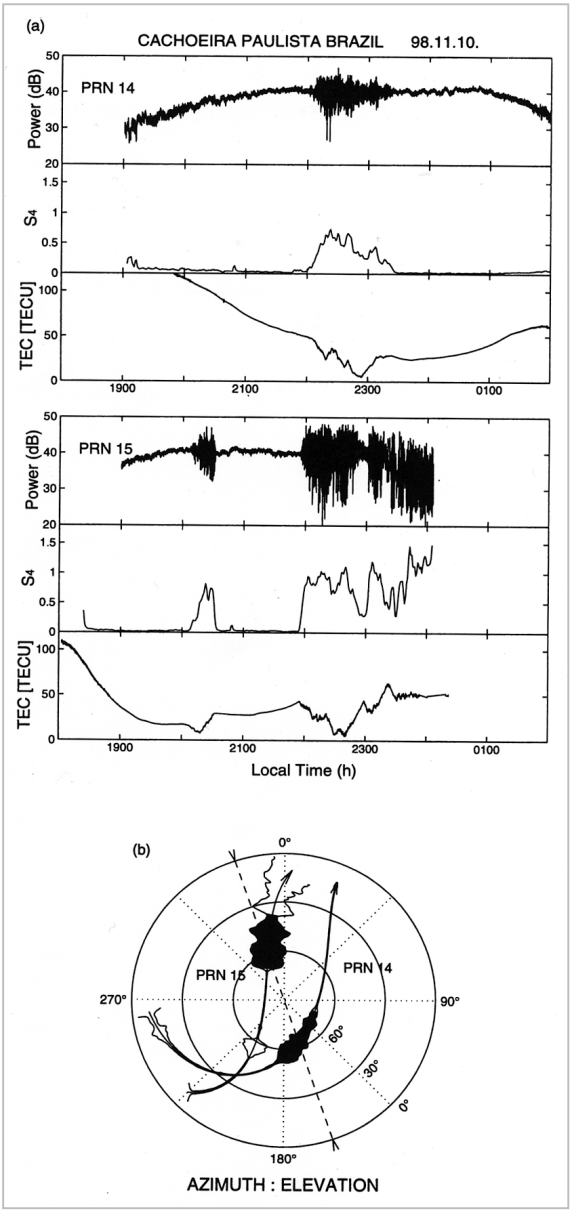

Fig.1 *Radio wave scintillations of GPS satellites and variations in total electron content (Kil et al.)*

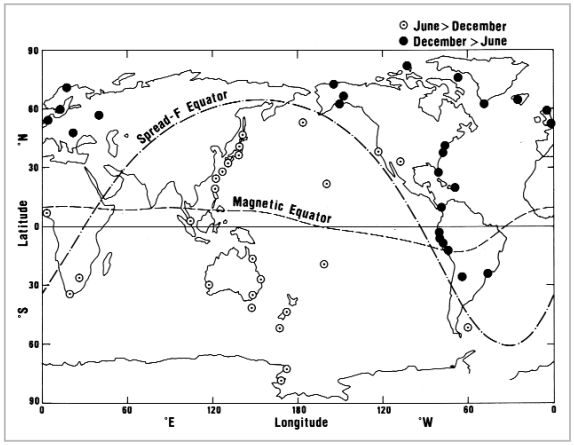

Fig.2 *Spread-F equator (adapted from Shimazaki)*

on annual variations in spread-F occurrences (Fig.2). The frequency of spread-F occurrences rises in June to the south of this spread-F equator and rises in December to the north. While most of this data came from the middle latitudes, it was believed that spread-F patterns could be extrapolated to equatorial regions. The theory behind the spread-F equator implies that the offset between the magnetic equator and the geographic equator should affect the occurrence of spread F. It took some time to realize that the offset is virtually negligible with respect to the spread-F mechanism.

The term "spread F" originates from the spreading of traces of F-region echoes on ionograms, strongly indicative of the deterioration of precision in determining the F-region critical frequency (foF2) read from normal echo traces. The spread of the traces results from the existence of several points that satisfy the conditions for producing echoes by specular reflection of sounding radio waves. In the past, researchers analyzed the spread F as indicators of spatial irregularities in the ionospheric structure. However, no clear standards existed for the notation "F" attached to the numerical values of foF2 in published ionospheric tables, which left room for personal interpretations of data readouts. Observatories might use different standards, preventing comparative analysis of the occurrence of irregularities on a global scale. The above idea of the spread-F equator appears to have been a stop-gap measure adopted under these circumstances.

2.1.1 Scintillation

The spread F results from ionospheric irregularities. A radio phenomenon resulting from the same irregularities is the scintillation of satellite radio waves. Radio waves in the VHF or microwave bands of frequencies far higher than foF2 experience phase advance, depending on the electron density of the ionosphere. When irregularities in the ionosphere distort the equi-phase surface of radio waves, the interference (Fresnel diffraction) causes

amplitude variations to be observed on the ground (Fig.3). Compared to the spread F, it is relatively easy to treat the variations in signal amplitude caused by scintillation both statistically and qualitatively. Thanks to the simple design of the scintillation observation instrument, both the data volume and reliability of statistical analyses have increased, along with increasing numbers of satellites available for the scintillation observation.

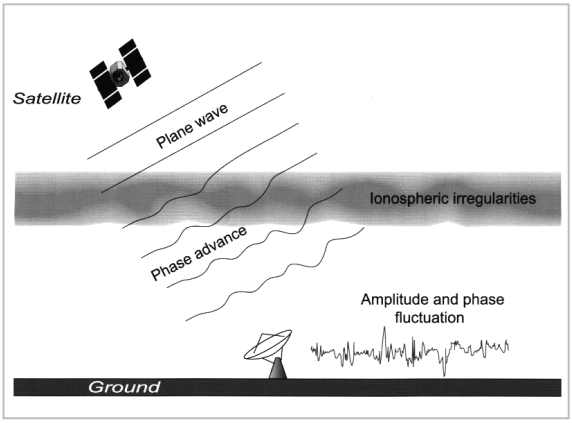

Fig.3 *Ionospheric scintillation*

2.1.2 Topside Sounding

The use of satellites in ionosphere studies has produced numerous results that contribute to the study of the irregularities. Results of observations by a series of satellites with topside sounders — the Alouette and ISIS — have shown that the spread F is not restricted to the bottomside, but is found even above the F region peak. The satellite observations have also shown high rates of occurrence near the equator and in the polar regions, with minimum rates of occurrence at middle latitudes. This observation of the topside spread F poses new questions regarding the mechanism of the irregularity evolution. Rayleigh-Taylor instability had been a strong candidate for the underlying mechanism, but this instability would require an electron density gradient anti-parallel to the direction of gravity. Rayleigh-Taylor instability could thus account only for the instability on the bottomside of the ionosphere. As evident in Fig.4, the morphological features of the latitudinal and local time variations in the spread-F frequencies are almost identical for ground-based and satellite observations (Calvert and Schmid, 1964). One point we note is that the morphology of the equatorial spread F clearly differs from those of other latitudes, suggesting that the mechanism of instability may be latitude-dependent. In the following sections, discussion will be focused on equatorial spread F.

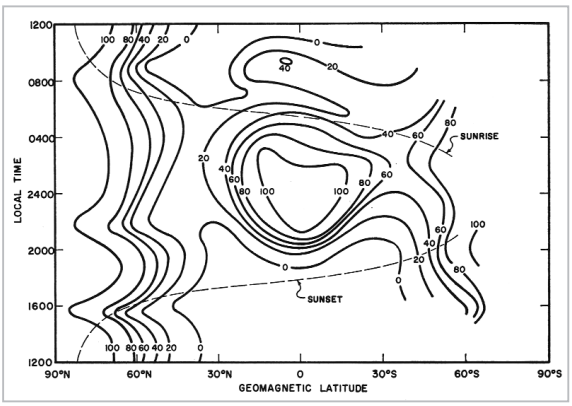

Fig.4a *Topside spread-F observed by the Alouette satellite (Calvert and Schmid)*

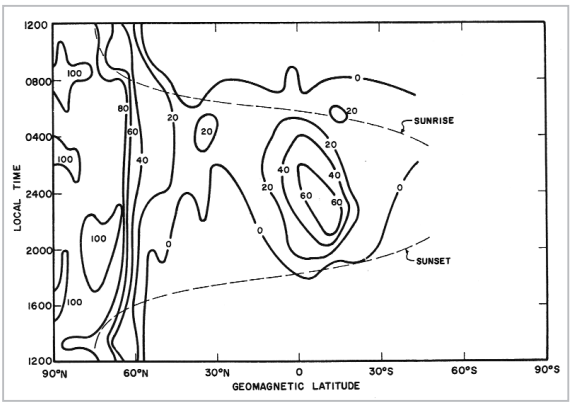

Fig.4b *Ground-based observation of spread-F (Calvert and Schmid)*

2.1.3 Radar Observations

Alongside satellites, a powerful tool for ionospheric studies is incoherent scatter (IS) radar. IS radars can observe signals scattered by individual electron in the ionosphere; the extreme faintness of these signals requires large observation facilities. At Jicamarca, Peru, located on the magnetic equator, the vertically directed radar beam is perpendicular to magnetic field lines; when spread F occurs during IS observation, coherent backscattering by irregularities generates strong signals that

may exceed IS signal levels by 40 dB, affecting the observations. The source of backscattering of this coherent echo is generated both above and below the F region peak nearly simultaneously. Haerendel (1973) attempted to explain this by Rayleigh-Taylor instability, proposing an L-shell direction gradient of total electron content (TEC) within the magnetic flux tube integrated along magnetic field lines, instead of a local vertical electron density gradient. Since the length of the magnetic field line increases with its equatorial crossing altitude, the integrated electron content reaches a maximum far above the F region peak. It was shown that gravitational instabilities may exist in terms of integrated electron number even above the F region peak, which is stable in terms of local parameters. Haerendel's theory was later developed into a model to explain seasonal and longitudinal features of the equatorial spread-F occurrence frequencies (Maruyama, 1984), but this problem remained fundamentally unresolved until Woodman and LaHoz (1976).

2.2 Plasma Bubble

Among the numerous possible mechanisms of equatorial ionospheric instability, Rayleigh-Taylor instability had won wide support, due to its capability in accounting for many of the characteristics of spread-F occurrences. However, it could not account for one aspect: Why does the instability occur simultaneously both above and below the F region peak? After observing strong signals from spread F events inhibiting ionospheric IS observation with a wider dynamic range, Woodman and LaHoz (1976) processed the data to produce a range-time-intensity (RTI) diagram. The improved temporal and intensity resolutions and provided a clearer image of the dynamic process of the irregularity evolution, in which the irregularity produced at the bottomside of the ionosphere rose within several minutes to an altitude of 1,000 km, passing through the F region peak in the process (Fig.5).

The signals directly observed by the radar are those reflected by Bragg scattering by field-aligned irregularities (FAI) and correspond to the 3-m structural components perpendicular to the magnetic field lines, equivalent to half the wavelength of the transmitted signal. Normally, such irregularities are not thought to be formed directly in the ionosphere, but are secondary instabilities at the wall of steep electron density gradients on a larger scale (when it is considered that the instabilities creating such large-scale electron density gradients are a primary phenomenon). Woodman and LaHoz assumed a nonlinear evolution of Rayleigh-Taylor instability based on the dynamic echo map, claiming that when the density difference between the low-density region of fluctuation in the ionosphere and the surroundings becomes sufficiently large, the

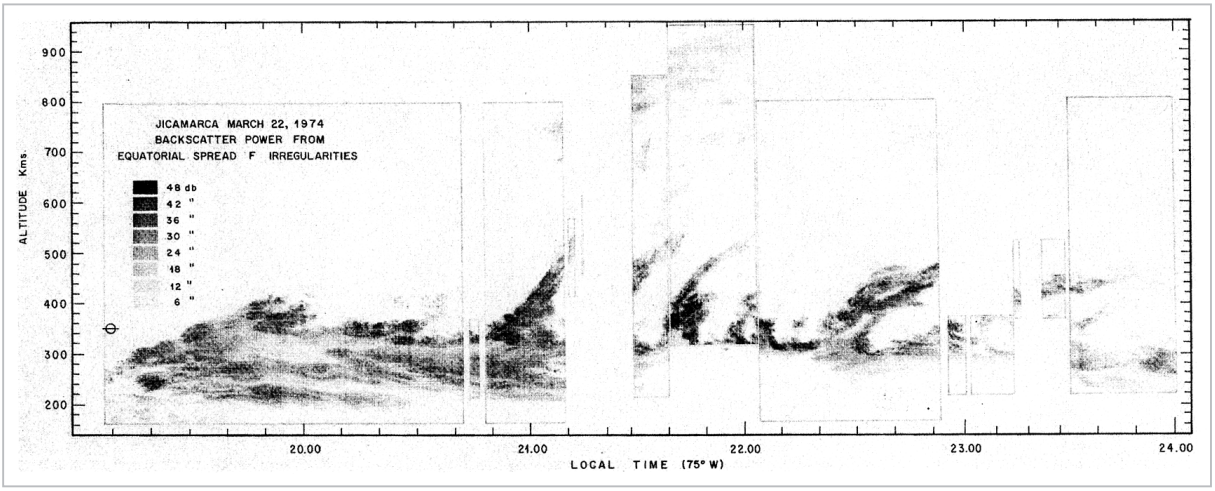

Fig.5 *Spread-F observed by Jicamarca radar (Woodman and LaHoz)*

low-density region will form a bubble and continue to rise, regardless of the background density gradient (which is downward in the topside ionosphere) (Fig.6). This structure is referred to as the "plasma bubble."

Following their study, plasma bubbles, which had appeared only as strong irregularities in radar observations, were directly confirmed by satellite observation as regions of abrupt drop-out of electron density by two orders of magnitude with dimensions of several tens of kilometers (Fig.7 : McClure et al., 1977). This finding was followed by computer simulations of the nonlinear evolution of the plasma bubble and observations of large-scale low-electron-density regions by optical instruments. Studies of plasma bubbles advanced rapidly thereafter.

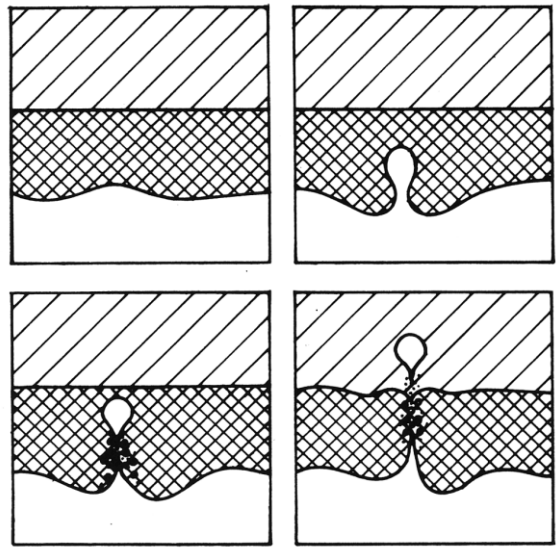

Fig.6 *Concept of plasma bubble (Woodman and LaHoz)*

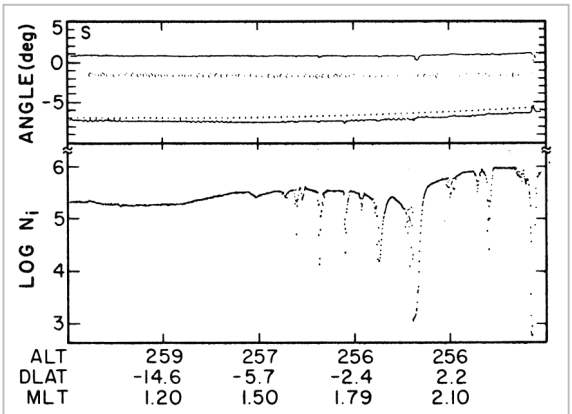

Fig.7 *In-situ observation of plasma bubble by the AE-C satellite (McClure et al.)*

2.3 The Rayleigh-Taylor Instability

Fig.8 is a schematic diagram of plasma instability at the bottomside of the ionosphere at the magnetic equator. Since the magnetic field lines are oriented horizontally northward and the F region plasma can be approximated as having a uniform distribution along the field line due to diffusion on the magnetic equator, this system can be represented fairly well by a 2-D approximation on a vertical E-W plane containing the equator. Fig.8 shows the eastward electric current generated by the difference in gravitational forces acting upon electrons and ions. Suppose that a small density fluctuation is produced on the bottomside of the ionosphere for some reason, causing an undulation of the isodensity surface.

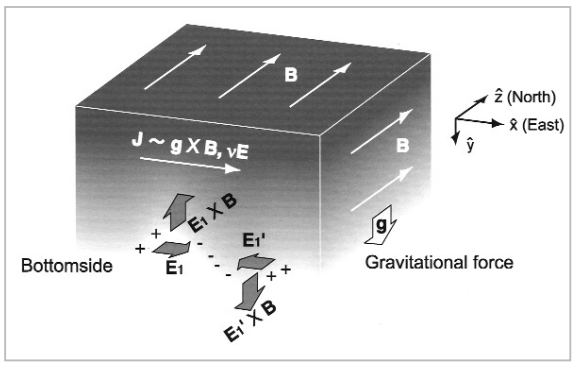

Fig.8 *Rayleigh-Taylor instability*

Since ions transport the aforementioned electric current, electron and ion isodensity surfaces become separated, resulting in local positive or negative charge buildup. These localized polarization electric fields have eastward and westward orientations in low-density and high-density regions, respectively, so the E × B drift due to this polarization field will be upward and downward in the low-density and high-density regions, respectively. As a result, density fluctuation is amplified. This condition is called plasma instability. Although details of the derivation will be omitted here, the growth rate (γ) of the instability in a linear regime can be expressed by the following

equation:

$$\gamma = -\frac{g}{\nu_{in}} \frac{1}{n_{i0}} \frac{\partial n_{i0}}{\partial y} \qquad (1)$$

Here, g is gravitational acceleration, ν_{in} the ion-neutral collision frequency, and n_{io} the background electron density. The y-axis is positive in the upward direction. This equation states that when the gravitational force and the electron density gradient are anti-parallel, i.e., on the bottomside, the growth rate is positive (note the negative sign on the right-hand side of the equation) and that its magnitude is proportional to density gradient.

Since the density gradient reverses above the F region peak, the fluctuation does not grow and the ionosphere becomes stable. The density gradient on the very bottom of the F region rapidly steepens due to recombination at the bottommost region after the ionization reaction ceases at sunset. The plasma bubble is thus essentially a nighttime phenomenon. The term for gravitational effects contains the ion-neutral collision frequency in its denominator, which is determined by the vertical profile of the neutral atmosphere. As the ion-neutral collision frequency decreases with altitude, the ionosphere becomes more unstable when the layer is high.

So far, we have dealt with electric currents generated by gravity. But instabilities also develop in a similar manner for electric currents generated by other causes. The Pedersen current due to the eastward electrical field generated by the dynamo effect and the effect of the collision between the neutral particles and ions in the downward neutral winds can both be treated similarly mathematically. The instability growth rate including the Pedersen current is given by the following equation:

$$\gamma = -\left(\frac{E_0}{B} + \frac{g}{\nu_{in}}\right) \frac{1}{n_{i0}} \frac{\partial n_{i0}}{\partial y} \qquad (2)$$

The additional term for the Pedersen current results in a positive growth rate when the electrical field is eastward. At the same time, the E × B drift by this electrical field pushes the region upward. In other words, the eastward electrical field contributes to the acceleration of instability growth, not only through the Pedersen current term, but also by amplifying the gravitational term by upwelling in the region. This effect is most pronounced immediately after sunset, when the eastward electric field is strengthened (evening enhancement).

2.4 Evening Enhancement

The motion of the equatorial ionosphere due to the E × B drift is generally upward in daytime and downward in nighttime. This electrical field is produced by the dynamo effect of E-region neutral winds. At dusk, the upward drift velocity increases for 1—2 hours prior to the drift reversal. This is called the evening enhancement, or prereversal enhancement, of the equatorial ionospheric electrical field. The essential characteristics of the evening enhancement are known to be the result of the dynamo effect by F-region neutral winds and the effect of rapid changes in E-region electric conductivity at sunset. Fig.9 gives a simplified explanation of the F-region dynamo. The thermospheric neutral winds at altitudes of the equatorial F-region near dusk blow eastward. The eastward motion of neutral particles causes only ions to drift upward by collision; the electric field produced by the charge separation is projected onto the E region through magnetic field lines with high electric conductivity. However, since the F-region dynamo is a constant current source with high internal resistance, it is readily short-circuited by the E-region with high Pedersen conductivity before sunset. At night, conductivity is reduced by the decrease in E-region electron density, creating a downward electrical field in the F region. The E × B drift induced by this electrical field has the same direction as thermospheric winds. At the boundary of daytime and nighttime conditions, the electrical field created by the F-region dynamo effect results in a non-uniform E-W distribution of electric conductivity in the E region, causing charge separation. Projected back onto the F region, the resulting

electrical field is eastward and westward to the west and east of the boundary. In other words, the eastward electrical field is intensified immediately before the reversal of the electrical field drift.

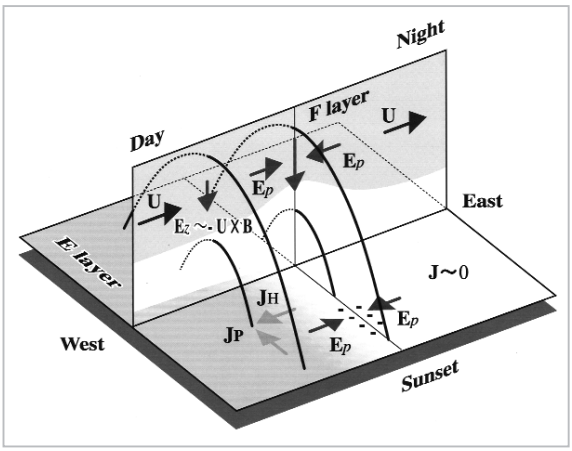

Fig.9 *Evening enhancement of the equatorial ionospheric electrical field by the F-region dynamo*

In the actual ionosphere, the ion density and collision frequency display altitude variations, and the condition of the E region projected along magnetic field lines varies with latitude. As a result, an EW drift component is added to the simple change in vertical drift.

Recent studies indicate that this creates a plasma vortex in the equatorial vertical plane. As will be stated later, it has been suggested that this plasma vortex may play an important role in the formation of plasma bubbles (Maruyama et al., 2002).

2.4.1 Observations

Among several methods for observation of the evening enhancement of the equatorial electric field, the most reliable technique might be IS radar, which measures the Doppler shifts of signals scattered by individual electrons. This makes it possible to obtain the altitude profiles of drift velocities when electron density is sufficiently high. However, the only IS radar positioned on the equator at this time is located in Jicamarca. Since the magnetic equator in Peru is greatly offset to the south, Jicamarca is not necessarily a general equatorial observation point. Drift behavior may vary significantly at other longitudes.

In-situ observations by low-orbiting satellites equipped with sensors such as ion drift meters have the advantage of being able to acquire data at all longitudes. But due to the rotational properties of the orbital plane, it is difficult to separate the components of local-time variations from seasonal variations. A simpler method is to estimate the drift from changes in F-region altitude by ionosonde measurements. However, since the F-region altitude is determined both by ionospheric motions and by chemical reactions such as ionization and recombination, the latter effects must be removed. Furthermore, apparent altitude (h'F), immediately scaled from ionograms, includes the effects of propagation delay by electron density distribution below the reflection points. In general, it is difficult to extract E × B drifts from the scaled data. However, after sunset, when the bottomside of the ionosphere rapidly disappears, and when the F region is located above a certain altitude, the effects of chemical reactions and delay can be ignored. The time derivative of h'F can then be considered to be equivalent to E × B drift.

Various observations have revealed that the amplitude of the evening enhancement displays very large variations, showing a strong correlation with solar activity. It amounts to several 10 m/s during solar maximums, while falling to near zero during solar minimums. It also exhibits different seasonal variation at different longitudes. These variations are seen not only in amplitude, but also in local times of the peak. In the case of Jicamarca in Fig.10, the drift velocities of the peak are highest at the spring and autumn equinoxes, followed by a large enhancement in December. They are weakest in July (Fejer et al., 1979).

3 Unresolved Problems

In the previous section, it was described that the equatorial spread F that causes strong scintillations in satellite radio is plasma bubbles formed by nonlinear development of

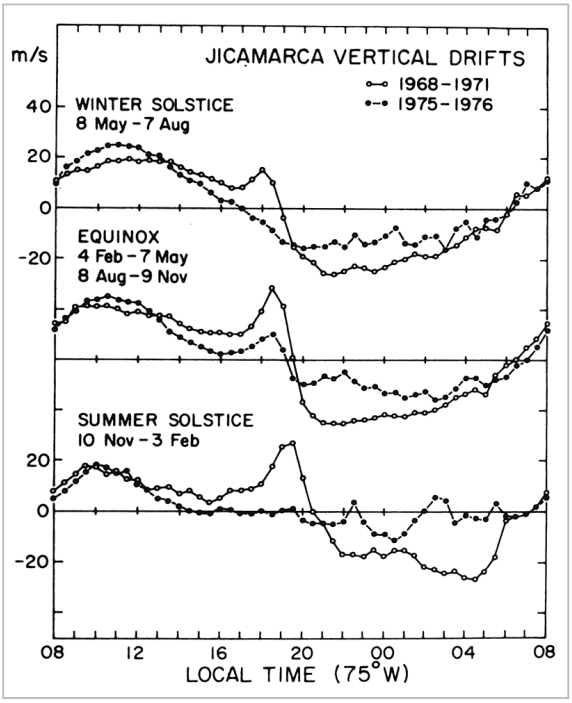

Fig.10 *Ionospheric vertical drift on the magnetic equator (Fejer et al.)*

Rayleigh-Taylor instability. However, as with other subjects in Space Weather, it is impossible to predict immediately the formation of a plasma bubble only when its basic mechanism is clarified. Below, we will discuss problems that remain before such predictions are possible. Of the several levels in the prediction process, the most elementary step is clarifying the statistical behavior (morphology) of plasma bubbles for as many parameters as possible. This should lead to an empirical model of plasma bubble formation and should also provide valuable insights into the various phenomena controlling its formation.

3.1 Seasonal and Longitudinal Variations

Since the days of IGY, the general features of the seasonal variations of the equatorial spread F, or plasma bubbles, have been known, based on data from scattered ground stations (Fig.2). Satellite observations clearly reveal their structure on a global scale.

Topside sounding by the ISS-b satellite was the first to show that seasonal and longitudinal controls were systematically present in its formation (Maruyama and Matuura, 1984). Until then, results of observation from the uneven distribution of observation points had led to the belief that the NS offset of the magnetic equator from the geographic equator plays some role in the longitudinal characteristics of the equatorial spread F. The results of satellite observations showed there were no clear differences between the seasonal characteristics of the equatorial spread F onset to the east and west of the longitude where the magnetic equator transects the geographic equator. Ironically, the intersections of the two equators are positions in the central parts of the Atlantic and Pacific Oceans. The lack of observation stations in these areas had long left the simple morphology unresolved.

As shown in Fig.11 by the dash-dotted line, the magnetic equator has the maximum southern offset in South America, transects the geographic equator above the Atlantic, and is then offset to the north on the African continent. In other words, the magnetic declination angle is greatest at the intersection of the two equators, approximately 20˚W above the Atlantic Ocean. At this longitude, the equatorial spread F, or plasma bubble, attains a maximum during northern winter (December) and a minimum during northern summer (June) (Fig.12). In contrast, in the Pacific Ocean, the magnetic equator transects the geographic equator from the north to south along the west-east longitudinal axis. Here, the maximum magnetic declination angle is approximately 15˚E. Subsequently, plasma bubble formation peaks in northern summer (June) and declines to a low in northern winter (December). Whilst, the magnetic equator runs nearly parallel 10˚ north of the geographic equator from the Indian Ocean to Asia. This results in a small magnetic declination angle, with the magnetic meridian plane aligned along a North-South axis. The corresponding plasma bubble formation annually has two maximums, around the spring and autumn equinoxes.

Although the space is often likened to a plasma experiment laboratory, it does not permit control of experimental parameters. Nev-

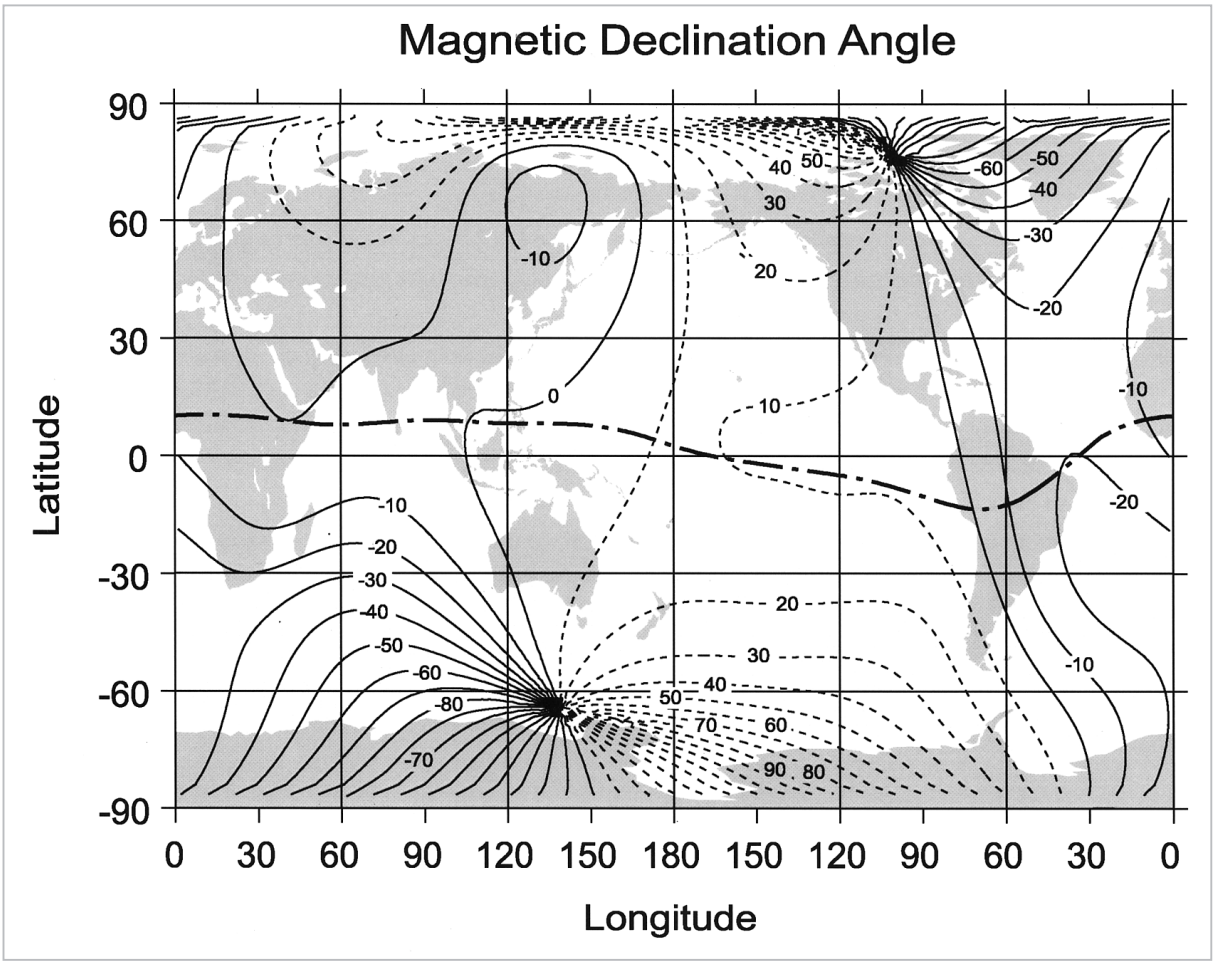

Fig.11 *Magnetic Declination Angle according to the IGRF model*

ertheless, by utilizing the systematic variations in atmospheric parameters by season and longitude, it is possible to search for ionospheric instabilities under conditions of varying parameters. Seasonal and longitudinal characteristics provide not only statistical probabilities for scintillation occurrences, but also help reveal the mechanism controlling the instabilities. If, as stated above, the variations in seasonal characteristics by longitude result from differences in magnetic declination angles, variations in thermospheric wind patterns is likely a cause of seasonal variations. The thermospheric winds at F region altitudes immediately after sunset are close to due eastward; the seasonal component flowing from the summer to winter hemisphere is added to this wind. If the seasonal component is considered to be zero at the spring and autumn equinoxes, the wind vector and magnetic meridian plane should be mutually perpendicular at longitudes with small magnetic declination angles. This means that the wind component that moves the plasma along magnetic field lines within the magnetic meridian plane vanishes. According to calculations by Maruyama (1988), when thermospheric winds have a strong NS component within the magnetic meridian plane, the ionospheric layer altitude decreases in the downwind hemisphere, accompanied by an increase in Pedersen conductivity. Since the polarization electrical field generated at the bottomside of the equatorial F region plays an important role in Rayleigh-Taylor instability, instability is suppressed when this electrical field is mapped along the magnetic field lines onto low-altitude F regions and the E regions that are displaced from the equator and is short-circuited there. The results of calculation of the insta-

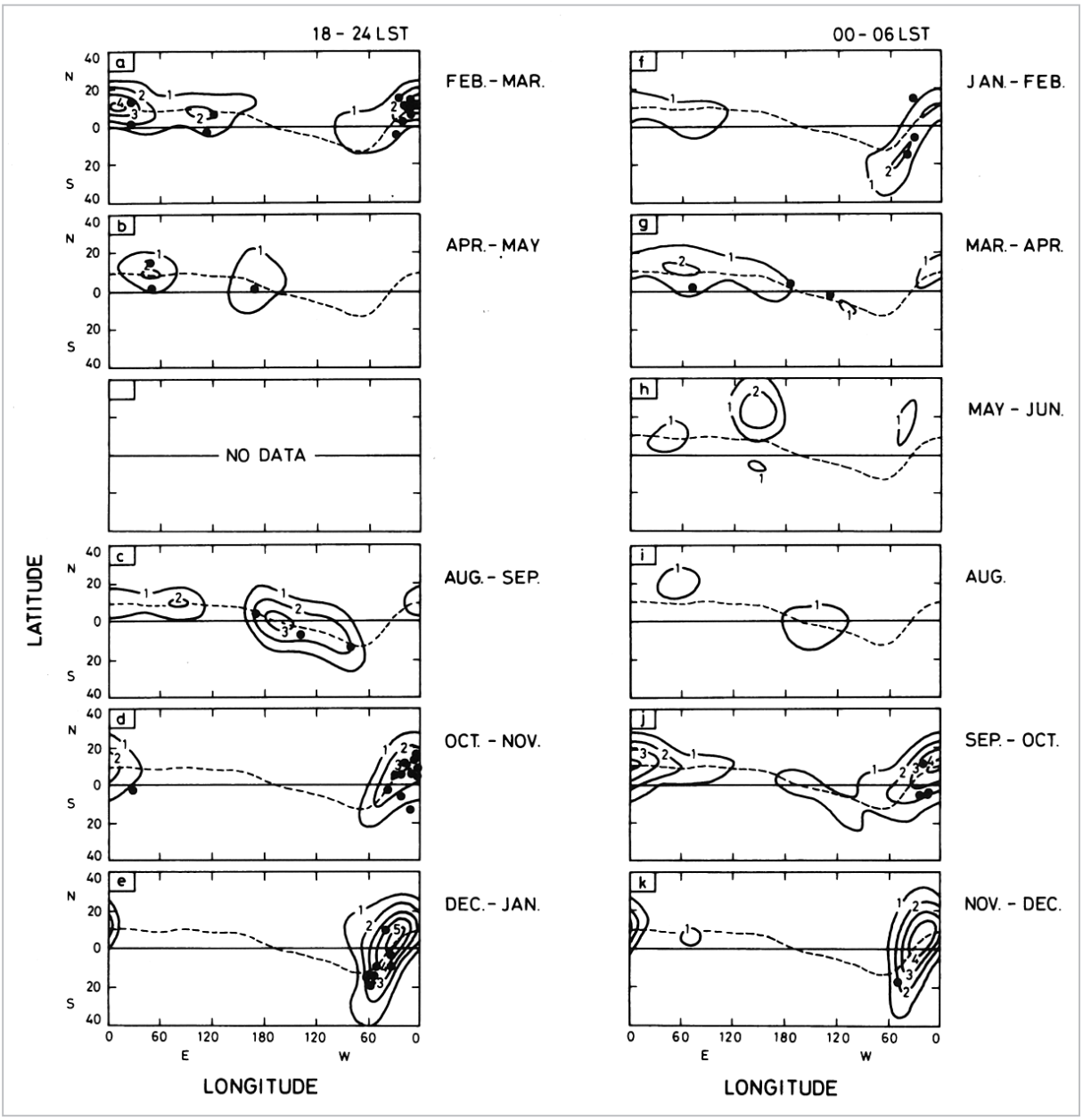

Fig.12 *Seasonal and longitudinal variations of topside spread-F by satellite observation (Maruyama)*

bility growth rate can explain changes in plasma bubble formation quantitatively. The actual electron density distribution at satellite altitudes determined from topside ionograms of the ISS-b satellite displays strong NS asymmetry in seasons and longitudes with abundant plasma bubble formations, confirming the instability suppression effect of the transequatorial winds.

Mendillo et al. (1992) offers the theory that the instability suppression effect of the transequatorial thermospheric wind incorporated to explain statistical seasonal and longitudinal variations may also be applied to explain the day-to-day variations that will be described in the next section. They found a correlation between the existence of transequatorial winds deduced from airglow observations and the results of scintillation observations. However, the results of other observations indicate no such connection, and no conclusion has been reached regarding the effect of transequatorial winds in suppressing plasma bubble formation. Resolving this uncertainty

will require case studies of the correlation between thermospheric winds and occurrences of irregularities for individual events, not statistical analysis. Abdu et al. (2001, personal communication) installed various observation instruments at magnetic conjugate points in Brazil to initiate observations of both the neutral atmosphere and plasma.

3.2 Day-to-day Variability

Plasma bubble formation is known to display large day-to-day fluctuations, even in conditions of latitudes and seasons of high statistical activity. The evening enhancement in vertical plasma drift, which theory suggests is an important condition for bubble formation, also displays large day-to-day variations. If the variations in bubble formation are consequences of variations in evening enhancement, we should find a strong positive correlation between vertical plasma drift velocity and equatorial spread F on a day-to-day basis. But according to Abdu et al. (1983), the correlation between the two is weak, as shown in Fig.13. This should be regarded as indicating the lack of a clear threshold value for bubble formation, implying that some other factor controls bubble formation, besides the evening enhancement. The key to predicting equatorial spread F onset lies in resolving this problem. As stated previously, the instability suppression effect of the transequatorial wind is a strong candidate as the causal factor of day-to-day variation.

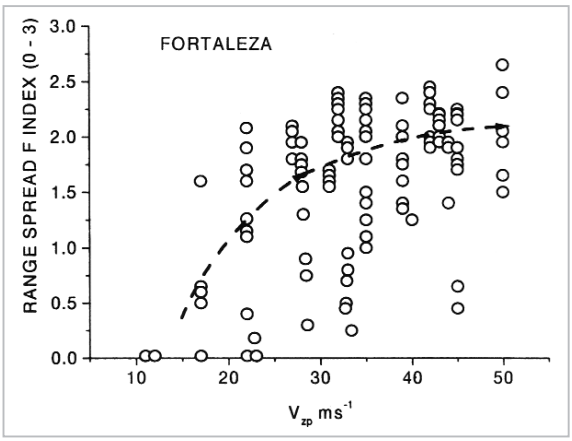

Fig.13 *Onsets of equatorial spread-F and vertical drift velocities (Abdu)*

The following other candidate for causal factors of day-to-day variations can be inferred from the onset time of bubbles, as shown in the following section.

4 Timing of Bubble Onset

Rayleigh-Taylor instability successfully explains many features of spread F, but there exist several contradictions between the theory and observations. One is the timing of bubble onset. According to the theory, since the ionosphere becomes unstable when conditions of strong eastward electrical field and high ionospheric layer altitude are satisfied, the instability must somehow correlate with the electrical field and layer altitude. The theory predicts that instability peaks when the electric field is eastward and the layer is high, or immediately before the ionosphere reaches its maximum altitude. With the reversal of the electrical field, the E × B drift instability term should suppress instability. However, observations often show the onset of a new plasma bubble when the layer falls.

Analyzing the precise timing of bubble onset based on radar observation data at Jicamarca, Kelley et al. (1981) reported the occurrence of spatial resonance when the phase velocity of the eastward-propagating atmospheric gravity waves coincides with the eastward plasma drift velocity, and that this results in significant amplification of variations in ionosphere layer altitude. They also showed that if we consider the instability term due to ion-neutral collision in a steep EW electron density gradient, the instability growth rate increases when the layer altitude falls as follows. When the drift direction reverses above the point considered, the layer altitude to the west is lower than that point for eastward-propagating waves, resulting in a westward electron density gradient at a given altitude. Since the thermospheric wind is eastward after sunset and the force due to collision is anti-parallel to the electron density gradient, conditions identical to gravitational instability are created. In other words, seeding by atmospheric gravity

waves, which vary day by day, may be one candidate for the cause of the variability.

The ionospheric layer altitude variation in the case analyzed by Kelley et al. (1981) differs from normal evening enhancement in that ascent and descent for two cycles are present and that similar ionospheric layer motions with shifted phase are present in the ionosphere data observed at Huancayo nearby. While this evidence indisputably points to a wave phenomenon (Fig.14), bubbles form during the descent phase of the layer altitude, even in a normal evening enhancement that cannot be identified as a wave phenomenon.

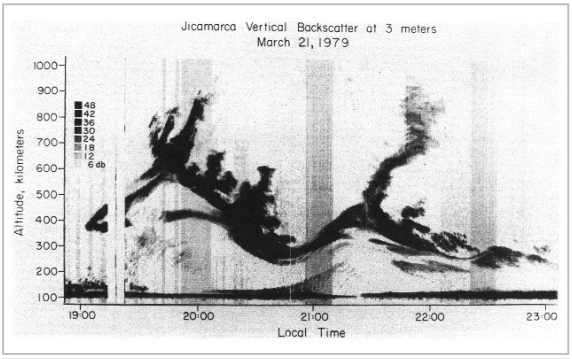

Fig.14 *Modulation of the equatorial ionosphere altitude by spatial resonance (Kelley et al.)*

Since evening enhancements are structures with time spans on the order of 1—2 hours, the spatial scale is around 1,500—3,000 km if the phenomenon is assumed to be fixed in local time, moving west. In such cases, the production of steep EW electron density gradients such as for atmospheric gravity waves cannot be expected. Maruyama et al. (2002) report a case in which the behavior of the ionospheric layer altitude differs for 2 points located on slightly different latitudes and on the same meridian for an equatorial spread F event. They conclude that a reversal of the vertical drift motion can be identified at a certain altitude when the vertical plasma motions at these 2 sites are projected onto the magnetic equator along magnetic field lines. Since plasma at F region altitudes is incompressible in the direction perpendicular to magnetic field lines, the EW plasma drift must also be taken into consideration. The drift vortex structure shown in Fig.15 was constructed on the assumption that the local time variations of drift are equivalent to longitudinal variations (spatial structure) at a given moment in time. If the EW drift shear is assumed to descend with time, the low altitude region of a later local time (LT), i.e., the low electron density region, should drift westward along the shear at the bottomside of the shear. In contrast, at the topside of the shear, the high electron density region should drift eastward, producing a steep vertical electron density gradient and increasing instability. In such cases, observations of high-density regions at the top of the shear should be able to identify bubbles formation during the descent phase of the ionosphere layer altitude.

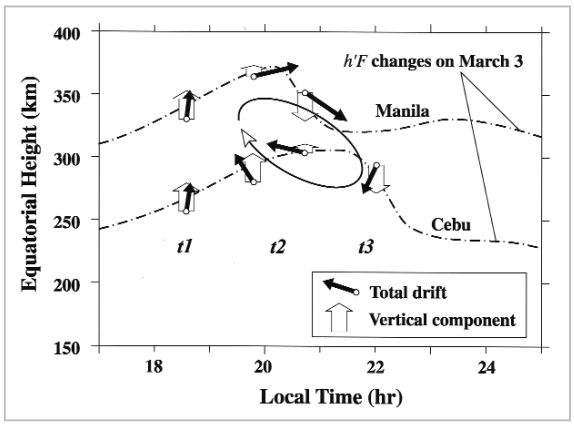

Fig.15 *Plasma vortex inferred from ionosonde observations (Maruyama et al.)*

The relationship between the plasma vortex and the Rayleigh-Taylor instability accompanying evening enhancement remains hypothetical and needs to be confirmed by observations. However, details of the vortex, an ionospheric phenomenon receiving widespread attention in recent years, are delineated through recent observations at Jicamarca (Kudeki and Bhattacharyya, 1999). Recent theoretical studies have successfully reconstructed the vortex (Haerendel et al., 1992). However, it remains to be seen whether the vortex is essentially detailed structures of evening enhancement and whether it always exists associated with evening enhancement. The final candidate for the causal factor of

day-to-day variability is the vortex accompanying evening enhancement.

4.1 Summary of Problems to Be Solved

Seasonal and longitudinal characteristics, local time characteristics, and correlation with the ionosphere layer altitude of the equatorial spread F, or the plasma bubble formation, have been confirmed statistically. But the key to predicting scintillation events lies in resolving the mechanism of the day-to-day variations of spread F, which is one of its primary characteristics. The following problems remain to be solved:

- The effect of Rayleigh-Taylor instability suppression by transequatorial thermospheric winds
- The EW electron density gradient created by eastward-propagating gravity waves and spatial resonance of plasma
- Steep vertical electron density gradient attained by the plasma vortex

In addition, it is important to realize the prediction of the ascent of the ionospheric layer altitude, or the variations in evening enhancement, the major prerequisite for the Rayleigh-Taylor instability.

Statistical analyses of a collection of numerous phenomena are virtually useless in solving these problems. Efforts need to be directed toward simultaneous observations of various physical quantities for individual events. The next section will introduce an observation project currently being planned at the CRL.

5 Observation Project

5.1 Effects of Transequatorial Winds

Since, in most cases, ground-based measurements of thermospheric winds are based on optical observations, such methods are highly vulnerable by meteorological conditions, and are not always easy to perform. Furthermore, since the subject latitude range extends to 10° on either side of the magnetic equator, multiple observation stations are required. Since thermospheric winds indirectly affect instability suppression through modification of electron density distribution, measurement of the winds themselves is not necessarily required.

Measurements of NS asymmetry on both sides of the magnetic equator may provide information on the transequatorial winds. In our project, ionosondes will be installed at magnetic conjugate points on the same magnetic meridian for ionosphere height observations.

Also, signals from GPS satellites will be received along with the ionosonde observation to observe the total electron content (TEC). Since the ionosphere ascends and descends along magnetic field lines in the equator-ward wind and pole-ward wind regions of the transequatorial winds, respectively, winds can be estimated by comparing the h'F values read directly from ionograms after sunset, when the lowermost part of the ionosphere has become rarefied through recombination. A similar NS asymmetry is also seen in TEC, but its relation to transequatorial winds is not so simple, since it is also dependent upon the distance from the equator due to the combined effects of transport of plasma across the equator and the recombination. It is also believed that the effects of transequatorial winds create the NS gradient of TEC just on the magnetic equator. Numerical modeling might assist interpretation of observed TEC data. Vertical $E \times B$ drift can be estimated from ionosonde observations on the magnetic equator, which should make interpretation of magnetic conjugate point data more certain. The onsets of instability development are confirmed from spread F traces in the ionograms and scintillations of GPS radio waves.

Magnetic conjugate point observations can only be made on limited meridians over the Earth's surface. In Brazil, South America, regions north of the magnetic equator are mostly covered by the jungles of Amazon, making observations in the area difficult. Similarly, for points south of the magnetic equator along the Peruvian coastline, corresponding conjugate points to the north would be located in the Andes. In India, the region

south of the magnetic equator is the Indian Ocean. In Africa, it is the desert region. In all these regions, there exists great difficulties to set up observation facilities at both magnetic conjugate points. However, several pairs can be constructed in Southeast Asia. Of these, the CRL has selected the 100˚E meridian plane. On this meridian, the magnetic equator passes through northern Phuket Island in Thailand. If an observation point is chosen in the Sumatra Island of Indonesia; the northern conjugate point will be located in northern Thailand, where several cities are located. Kyoto University already has an Equatorial Atmosphere Radar (EAR) facility in Koto Tabang of Sumatra Island; CRL will install an ionosonde nearby in collaboration with Indonesian and Japanese research groups. Lampang in northern Thailand is near the corresponding northern magnetic conjugate point. An ionosonde will be installed there in collaboration with Chiang Mai University. The Chumphon campus of King Mongkut's Institute of Technology Ladkrabang (KMITL) is located in Chumphon, near the magnetic equator. An ionosonde is currently being installed there in collaboration with the KMITL. Fig.16 and 17 show the proposed layout of the entire observation network.

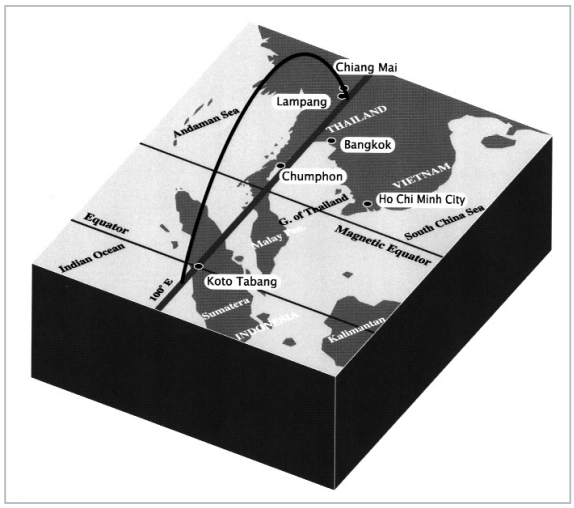

Fig.16 *North-South Conjugate Observation Project in Southeast Asia (1)*

5.2 Gravity Waves and Spatial Resonance

Observed as a temporal change of plasma drift velocity at fixed observation points on Earth, the evening enhancement produced by the F region dynamo is often assumed to be equivalent to the longitudinal spatial structure. That is, the vertical plasma drift pattern is thought to shift westward with the movement of the sunset terminator, although, such presumption must be confirmed by observation. When spatial resonance occurs between eastward-propagating gravity waves and plasma drift, the phase velocity is opposite to the movement of the sunset terminator. Thus, the variation in ionosphere layer altitude caused by the two effects should vary significantly at different longitudes. Observations in southern part of Vietnam, which lies on the same latitude as the aforementioned Cumphon of the

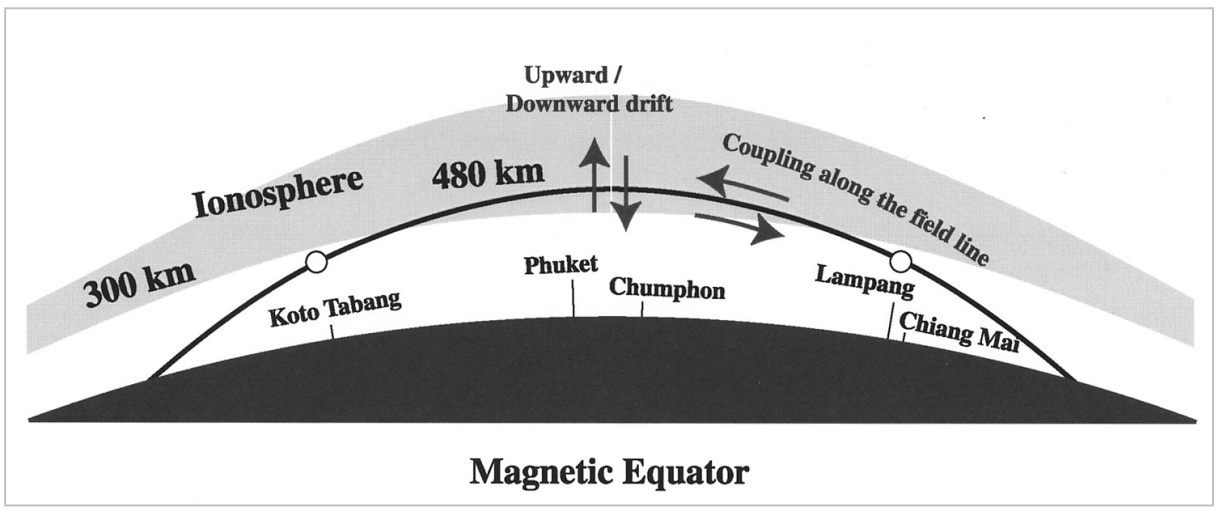

Fig.17 *North-South Conjugate Observation Project in Southeast Asia (1)*

100˚E ionosonde network, should be useful in investigating this phenomenon. An ionosonde has already been installed on Cebu Island in the Philippines, and observations are underway in collaboration with the University of San Carlos. An EW ionosonde network is expected to distinguish the structure propagating westward with the sunset terminator and the structure propagating eastward with the gravity waves.

Past studies of large-scale equatorial waves have included direction-finding observations of transequatorial propagating radio waves in the HF band between Tsumeb in Southwest Africa and Lindau, Germany. The method proved effective for remote sensing of equatorial ionospheric disturbances (Röttger, 1973). Such experiments normally use an antenna array to determine the angle of arrival based on the phase relationship among the received radio waves at each antenna and require unmodulated signals for observations. It may be difficult to install a transmitter dedicated to transequatorial propagation observation abroad, but if HF radio waves of overseas broadcasting can be utilized for the observation, it should satisfy the purpose in question with relative ease. With the cooperation of the Ministry of Public Management, Home Affairs, Post and Telecommunications, the CRL has conducted radio direction-finding experiments of radio waves transmitted by Radio Australia in Melbourne, Australia, at the radio monitoring facility in Togane City, Chiba prefecture.

This facility uses the MUSIC algorithm and is capable of monitoring the arrival angle of radio waves with any modulation. Fig.18 shows the results of this observation.

The points represent the azimuth angles of arrival waves second by second. The figure indicates that near sunset, the observed direction of propagation is offset westward from the original direction estimated from the great circle path, and that the observed direction eventually shifts eastward. This is followed by a new propagation path mode that begins in the west and shifts eastward over time. A separate mode is also seen that gradually returns to the original direction of propagation. Application of these methods to wave-like structure in the equatorial ionospher will require further analysis, combined with methods such as ray tracing, but the results of these experiments indicate the feasibility of applying this method to the remote sensing of the equatorial ionosphere using existing radio waves. A similar facility for scientific observation has since been set up at the Oarai test field of CRL, and preparations are underway to set up a full-time observation system. At the intersection of the Melbourne-Oarai propagation path and the magnetic equator is Yap Island of the Federated States of Micronesia. A portable ionosonde has been installed there, with plans for observations concurrent with transequatorial propagation observations.

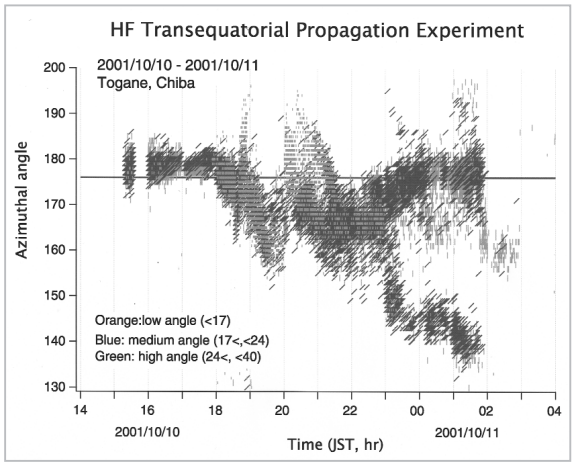

Fig.18 *Azimuthal angle variations in transequatorial propagation of radio waves*

5.3 Plasma Vortex

The original clue associating the variations in ionosphere layer altitude to spread F events was drawn from the results of observations at two points in the Philippines, at Cebu Island and Manila to the north. The latitudinal separation between the two points is 5˚. The magnetic meridian planes containing the two points are separated by 315 km along an EW axis. It was not quite possible to conclude whether the difference in ionosphere layer altitude at the two points was due to the differ-

ence in longitude or to waves propagating along the EW axis. The Thailand observation network should resolve this problem and provide new insights into the wider behavior of the plasma vortex itself, insights likely to extend beyond the association with plasma bubbles.

References

1 Abdu, M.A., R.T. Medeiros, J.A. Bittencourt, and I.S. Batista, "Vertical ionization drift velocities and range spread F in the evening equatorial ionosphere", J. Geophys. Res., Vol.88, pp.399-401, 1983.

2 Calvert, W. and C.W. Schmid, "Spread-F observations by the Alouette topside sounder satellite", J. Geophys. Res., Vol.69, pp.1839-1852, 1964.

3 Farley, D.T., E. Bonelli, B.G. Fejer, and M.F. Larsen, "The prereversal enhancement of the zonal electric field", J. Geophys. Res., Vol.91, pp.13,723-13,728, 1986.

4 Fejer, B.G., D.T. Farley, R.F. Woodman, and C. Calderon, "Dependence of equatorial F region vertical drift on season and solar cycle", J. Geophys. Res., Vol.84, pp.5792-5796, 1979.

5 Haerendel, G., "Theory of equatorial spread F", report, Max-Planck Inst. für Phys. Astrophys., Federal Republic of Germany, 1973.

6 Haerendel, G., J.V. Eccles, and S. Çakir, "Theory for modeling the equatorial evening ionosphere and the origin of the shear in the horizontal plasma flow", J. Geophys. Res., Vol.97, pp.1209-1223, 1992.

7 Kelley, M.C., M.F. Larsen, C. LaHoz, and J.P. McClure, "Gravity wave initiation of equatorial spread F: A case study", J. Geophys. Res., Vol.86, pp.9087-9100, 1981.

8 Kil, H., P.M. Kintner, E.R. de Paula, and I.J. Kantor, "Global positioning system measurements of the ionospheric zonal apparent velocity at Cachoeira Paulista in Brazil", J. Geophys. Res., Vol.105, pp.5317-5327, 2000.

9 Kudeki, E. and S. Bhattacharyya, "Postsunset vortex in equatorial F-region plasma drifts and implications for bottomside spread-F", J. Geophys. Res., Vol.104, pp.28,163-28,170, 1999.

10 Maruyama, T., "A diagnostic model for equatorial spread F. 1. Model description and application to electric field and neutral wind effects", J. Geophys. Res., Vol.93, pp.14,611-14,622, 1988.

11 Maruyama, T. and N. Matuura, "Longitudinal variability of annual changes in activity of equatorial spread F and plasma bubbles", J. Geophys. Res., Vol.89, pp.10,903-10,912, 1984.

12 Maruyama, T., K. Nozaki, M. Yamamoto, and S. Fukao, "Ionospheric height changes at two closely separated equatorial stations and implications in spread F onsets", J. Atmos Solar-Terr. Phys., Vol.64, pp.1557-1563, 2002.

13 McClure, J.P., W.B. Hanson, and J.H. Hoffman, "Plasma bubbles and irregularities in the equatorial ionosphere", J. Geophys. Res., Vol.82, pp.2650-2656, 1977.

14 Mendillo, M., J. Baumgardner, P.I. Xiaoquing, and P.J. Sultan, "Onset conditions for equatorial spread F", J. Geophys. Res., Vol.97, pp.13,865-13,876, 1992.

15 Röttger, J., "Wavelike structure of large scale equatorial spread F irregularities", J. Atmos. Terr. Phys., Vol.35, pp.1195-1206 , 1973.

16 Scannapieco, A.J. and S.L. Ossakow, "Nonlinear equatorial spread F", Geophys. Res. Lett., Vol.3, pp.451-454, 1976.

17 Tsunoda, R.T., R.C. Livingston, and C.L. Rino, "Evidence of a velocity shear in bulk plasma motion associated with post-sunset rise of the equatorial F-layer", Geophys. Res. Lett., Vol.8, pp.807-810, 1981.

18 Woodman, R.F. and C. La Hoz, "Radar observations of F region equatorial irregularities", J. Geophys. Res., Vol.81, pp.5447-5466, 1976.

***MARUYAMA Takashi**, Ph. D.*

Leader, Ionosphere and Radio Propagation Group, Applied Research and Standards Division

Upper Atmosphere Physics